Available online at www.sciencedirect.com
SCIENCE DIRECT®
Composites: Part B 35 (2004) 591–598
composites Part B: engineering
www.elsevier.com/locate/compositesb

Elasticity, shell theory and finite element results for the buckling of long sandwich cylindrical shells under external pressure

Jea-Hyeong Han, George A. Kardomateas*, George J. Simitses

School of Aerospace Engineering, Georgia Institute of Technology, Atlanta, GA 30332-0150, USA

Received 11 June 2003; accepted 17 July 2003

Available online 9 April 2004

Abstract

The buckling of a sandwich cylindrical shell under uniform external hydrostatic pressure is studied in three ways. The simplifying assumption of a long shell is made (or, equivalently, 'ring' assumption), in which the buckling modes are assumed to be two-dimensional, i.e. no axial component of the displacement field, and no axial dependence of the radial and hoop displacement components. All constituent phases of the sandwich structure, i.e. the facings and the core, are assumed to be orthotropic. First, the structure is considered a three-dimensional (3D) elastic body, the corresponding problem is formulated and the solution is derived by solving a set of two linear homogeneous ordinary differential equations of the second-order in r (the radial coordinate), i.e. an eigenvalue problem for differential equations, with the external pressure, p the parameter/eigenvalue. A complication in the sandwich construction is due to the fact that the displacement field is continuous but has a slope discontinuity at the face-sheet/core interfaces, which necessitates imposing 'internal' boundary conditions at the face-sheet/core interfaces, as opposed to the traditional two-end-point boundary value problems. Second, the structure is considered a shell and shell theory results are generated with and without accounting for the transverse shear effect. Two transverse shear correction approaches are employed, one based only on the core, and the other based on an effective shear modulus that includes the face-sheets. Third, finite element results are generated by use of the ABAQUS finite element code. In this part, two types of elements are used: a shear deformable shell element and a solid 3D (brick) element. The results from all these three different approaches are compared.

Keywords: B. Buckling; B. Elasticity; A. Layered structures; C. Analytical modeling

1. Introduction

In composite structures, the buckling strength is an important design parameter because of the large strength-to-weight ratio and the lack of extensive plastic yielding. Often, these advanced materials are employed in a sandwich construction, which consists of two thin composite laminated faces and a thick soft core made of foam or low strength honeycomb. In sea navy applications, sandwich plate or shell structures are considered for surface ship substructures or submersible hulls. In these sandwich structures, the need for the accurate prediction of critical loads is even greater, because of the effect of the low modulus core, which promotes the transverse shear effects, and the comparatively large thickness of the structure.

Although structural buckling was traditionally studied using column, plate or shell theories, the demands and complexities of advanced composite and sandwich construction have brought to surface the inadequacy of these classical approaches. In response, the mechanics community has researched higher order theories, e.g. Refs. [1,2], which, nevertheless, are still based on a priori assumptions, made most commonly for the displacement distributions through the thickness. The need exists for assessing the accuracy of all these different approaches. A solution for the critical load based on considering the structure as a three-dimensional (3D) elastic body would serve as a benchmark.

In this regard, several elasticity solutions for monolithic homogeneous composite shell buckling have become available. In particular, Kardomateas [3] formulated and solved the problem for the case of uniform external pressure and orthotropic homogeneous material; in this study, just as in the present one, a long shell was studied

* Corresponding author.
E-mail address: george.kardomateas@aerospace.gatech.edu (G.A. Kardomateas).

1359-8368/$ - see front matter © 2004 Elsevier Ltd. All rights reserved.
doi:10.1016/j.compositesb.2003.07.002

('ring' assumption). The ring assumption was relaxed in a further study [4], in which a non-zero axial displacement and a full dependence of the buckling modes on the three coordinates was assumed. Elasticity solutions for other types of loading of homogeneous composite shells are summarized in Ref. [5].

The geometry of a circular cylindrical shell is particularly attractive for constructing elasticity solutions due to the axisymmetry which simplifies the analysis. Furthermore, a pre-requisite to obtaining elasticity solutions for shell buckling is the existence of 3D elasticity solutions to the pre-buckling problem. Elasticity solutions for monolithic homogeneous orthotropic cylindrical shells have been provided by Lekhnitskii [6]. Recently, elasticity solutions for sandwich shells were obtained by Kardomateas [7], by properly extending the solutions for monolithic structures. The latter is the pre-buckling solution needed to formulate the bifurcation problem in the elasticity context, as outlined in the present paper. The comparison to shell theory predictions will be based on the formulae presented in Refs. [8,9] and specialized to an infinite length cylinder, whose behavior is equivalent to that of a sandwich ring. Finally, a comparison is made with results from a commercial finite element code using both a shear deformable shell element and a solid 3D (brick) element.

2. Formulation

The buckling equations in the context of 3D elasticity for a cylindrical shell were obtained by Kardomateas [3] from the equations of equilibrium in terms of the second Piola-Kirchhoff stress tensor, by subtracting these at the perturbed and initial states, and making order of magnitude assumptions on the products of stresses and strains/rotations, based on the fact that a characteristic feature of stability problems is the shift from positions with small rotations to positions with rotations substantially exceeding the strains.

The associated boundary conditions were obtained from the traction (stress resultant) relationships in terms of the second Piola-Kirchhoff stress tensor, and by further considering the fact that because of the hydrostatic pressure loading, the magnitude of the surface load remains invariant under deformation, but its direction changes (since hydrostatic pressure is always directed along the normal to the surface on which it acts). Again, these were obtained in Ref. [3] by writing these equations for the initial and the perturbed equilibrium position and then subtracting them and using the previous arguments on the relative magnitudes of the rotations. These conditions will also be used when we impose traction continuity at the core/face-sheet interfaces.

2.1. Pre-buckling state

The problem under consideration is that of a sandwich hollow cylinder deformed by uniformly distributed external pressure, p (Fig. 1) and of infinite length (generalized plane deformation assumption). Then, not only the stresses, but also the displacements do not depend on the axial coordinate. Alternatively, this is the assumption we would make if the cylinder was securely fixed at the ends. An elasticity solution to this problem was provided by Kardomateas [7]. The solution is an extension of the classical one by Lekhnitskii [6] for a homogeneous, orthotropic shell and was provided in closed form. All three phases, i.e. the two face-sheets and the core were assumed to be orthotropic. Moreover, there were no restrictions as far as the individual thicknesses of the face-sheets and the sandwich construction could be asymmetric.

In this configuration, the axially symmetric distribution of external forces produces stresses identical at all cross-sections and dependent only on the radial coordinate r. We take the axis of the body as the z-axis of the cylindrical coordinate system and we denote by R_1 and R_2 the inner and outer radii. Let us also denote each phase by i where $i = f_2$ for the outer face-sheet, $i = c$ for the core and $i = f_1$ for the inner face-sheet. Then, for each phase, the orthotropic strain–stress relations are

$$\begin{bmatrix} \epsilon_{rr}^{(i)} \\ \epsilon_{\theta\theta}^{(i)} \\ \epsilon_{zz}^{(i)} \\ \gamma_{\theta z}^{(i)} \\ \gamma_{rz}^{(i)} \\ \gamma_{r\theta}^{(i)} \end{bmatrix} = \begin{bmatrix} a_{11}^i & a_{12}^i & a_{13}^i & 0 & 0 & 0 \\ a_{12}^i & a_{22}^i & a_{23}^i & 0 & 0 & 0 \\ a_{13}^i & a_{23}^i & a_{33}^i & 0 & 0 & 0 \\ 0 & 0 & 0 & a_{44}^i & 0 & 0 \\ 0 & 0 & 0 & 0 & a_{55}^i & 0 \\ 0 & 0 & 0 & 0 & 0 & a_{66}^i \end{bmatrix} \begin{bmatrix} \sigma_{rr}^{(i)} \\ \sigma_{\theta\theta}^{(i)} \\ \sigma_{zz}^{(i)} \\ \tau_{\theta z}^{(i)} \\ \tau_{rz}^{(i)} \\ \tau_{r\theta}^{(i)} \end{bmatrix}, \quad (i = f_1, c, f_2) \tag{1}$$

where a_{ij}^i are the compliance constants (we have used the notation $1 \equiv r$, $2 \equiv \theta$, $3 \equiv z$).

Let us introduce the following notation for constants which enter into the stress formulas and depend on the elastic properties:

$$\beta_{11}^i = a_{11}^i - \frac{(a_{13}^i)^2}{a_{33}^i}; \qquad \beta_{22}^i = a_{22}^i - \frac{(a_{23}^i)^2}{a_{33}^i} \quad (i = f_1, c, f_2), \tag{2a}$$

$$\beta_{12}^i = a_{12}^i - \frac{a_{13}^i a_{23}^i}{a_{33}^i} \qquad (i = f_1, c, f_2); \tag{2b}$$

$$k_i = \sqrt{\frac{\beta_{11}^i}{\beta_{22}^i}}; \qquad (i = f_1, c, f_2)$$

Then, the pre-buckling stresses in each of the phases, i.e. for $i = f_1, c, f_2$, are:

$$\sigma_{rr}^{0(i)}(r) = p(C_1^{(i)} r^{k_i - 1} + C_2^{(i)} r^{-k_i - 1}), \tag{3a}$$

$$\sigma_{\theta\theta}^{0(i)}(r) = p(C_1^{(i)} k_i r^{k_i - 1} - C_2^{(i)} k_i r^{-k_i - 1}), \tag{3b}$$

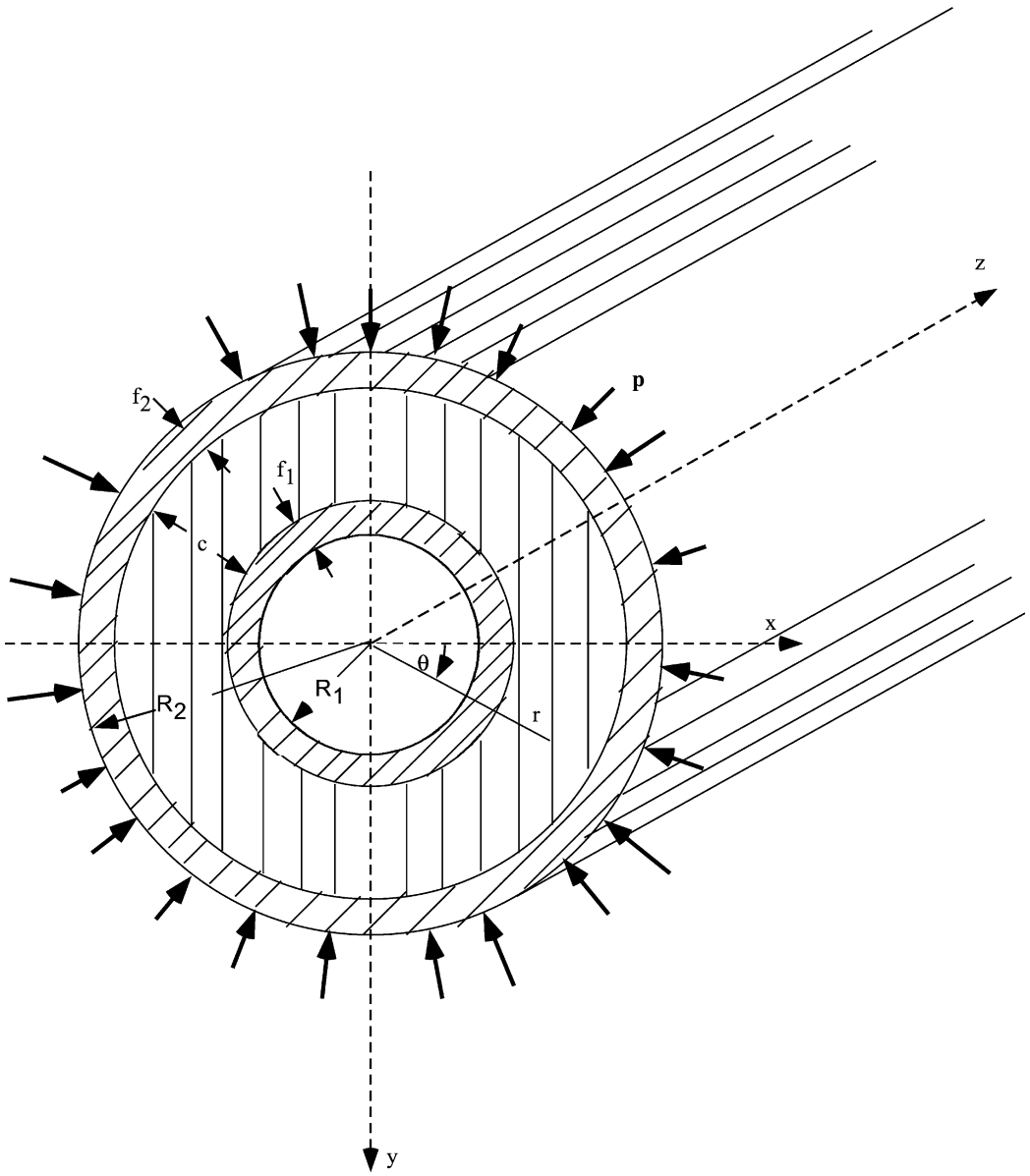

Fig. 1. Definition of the geometry and the loading. A cylindrical sandwich shell under external pressure.

$$\tau_{\theta z}^{0(i)}(r) = \tau_{rz}^{(i)}(r) = \tau_{r\theta}^{0(i)}(r) = 0, \tag{3c}$$

$$\sigma_{zz}^{0(i)}(r) = p\left\{-C_1^{(i)}\frac{(a_{13}^i + a_{23}^i k_i)}{a_{33}^i} r^{k_i - 1} - C_2^{(i)}\frac{(a_{13}^i - a_{23}^i k_i)}{a_{33}^i} r^{-k_i - 1}\right\}. \tag{3d}$$

Furthermore, the pre-buckling radial displacement is found to be

$$u^{0(i)}(r) = p\left[C_1^{(i)}\frac{(\beta_{11}^i + k_i\beta_{12}^i)}{k_i} r^{k_i} - C_2^{(i)}\frac{(\beta_{11}^i - k_i\beta_{12}^i)}{k_i} r^{-k_i}\right], \tag{3e}$$

the other displacements being zero, i.e. $v^{0(i)}(r) = w^{0(i)}(r) = 0$.

The constants $C_1^{(i)}$, $C_2^{(i)}$ are found from the conditions on the cylindrical lateral surfaces (traction-free) and the conditions at the interfaces between the phases of the sandwich structure. Specifically, the traction conditions at the face-sheet/core interfaces [7]

$$\sigma_{rr}^{(f1)}|_{r=R_1+f_1} = \sigma_{rr}^{(c)}|_{r=R_1+f_1}; \qquad \sigma_{rr}^{(c)}|_{r=R_2-f_2} = \sigma_{rr}^{(f2)}|_{r=R_2-f_2},$$

give two equations

$$C_1^{(f_1)}(R_1+f_1)^{k_{f_1}-1} + C_2^{(f_1)}(R_1+f_1)^{-k_{f_1}-1} = C_1^{(c)}(R_1+f_1)^{k_c-1} + C_2^{(c)}(R_1+f_1)^{-k_c-1}, \tag{4a}$$

and

$$C_1^{(c)}(R_2-f_2)^{k_c-1}+C_2^{(c)}(R_2-f_2)^{-k_c-1} = C_1^{(f_2)}(R_2-f_2)^{k_{f_2}-1}+C_2^{(f_2)}(R_2-f_2)^{-k_{f_2}-1}. \quad (4b)$$

The displacement continuity at the face-sheet/core interfaces, give another two equations

$$C_1^{(f_1)}\frac{(\beta_{11}^{f_1}+k_{f_1}\beta_{12}^{f_1})}{k_{f_1}}(R_1+f_1)^{k_{f_1}} - C_2^{(f_1)}\frac{(\beta_{11}^{f_1}-k_{f_1}\beta_{12}^{f_1})}{k_{f_1}} \times(R_1+f_1)^{-k_{f_1}} = C_1^{(c)}\frac{(\beta_{11}^{c}+k_c\beta_{12}^{c})}{k_c}(R_1+f_1)^{k_c} - C_2^{(c)}\frac{(\beta_{11}^{c}-k_c\beta_{12}^{c})}{k_c}(R_1+f_1)^{-k_c}, \quad (5a)$$

and

$$C_1^{(c)}\frac{(\beta_{11}^{c}+k_c\beta_{12}^{c})}{k_c}(R_2-f_2)^{k_c} - C_2^{(c)}\frac{(\beta_{11}^{c}-k_c\beta_{12}^{c})}{k_c} \times(R_2-f_2)^{-k_c} = C_1^{(f_2)}\frac{(\beta_{11}^{f_2}+k_{f_2}\beta_{12}^{f_2})}{k_{f_2}}(R_2-f_2)^{k_{f_2}} - C_2^{(f_2)}\frac{(\beta_{11}^{f_2}-k_{f_2}\beta_{12}^{f_2})}{k_{f_2}}(R_2-f_2)^{-k_{f_2}}. \quad (5b)$$

Finally, the conditions of tractions at the lateral surfaces (traction-free inner surface and pressure, p, at the outer) give:

$$C_1^{(f_1)}R_1^{k_{f_1}-1}+C_2^{(f_1)}R_1^{-k_{f_1}-1}=0, \quad (6a)$$

$$C_1^{(f_2)}R_2^{k_{f_2}-1}+C_2^{(f_2)}R_2^{-k_{f_2}-1}=-1. \quad (6b)$$

The six linear equations (4)–(6) can be solved for the six constants $C_1^{(i)}$, $C_2^{(i)}$, $(i=f_1,c,f_2)$.

2.2. Perturbed state

In the perturbed position, we seek plane equilibrium modes as follows:

$$u_i(r,\theta)=U_i(r)\cos n\theta; \qquad v_i(r,\theta)=V_i(r)\sin n\theta; \qquad w_i(r,\theta)=0; \qquad i=f_1,c,f_2 \quad (7)$$

Substituting these in the strain vs displacement relations

$$\epsilon_{rr}^{(i)}=\frac{\partial u_i}{\partial r}; \qquad \epsilon_{\theta\theta}^{(i)}=\frac{1}{r}\frac{\partial v_i}{\partial\theta}+\frac{u_i}{r};$$

$$\gamma_{r\theta}^{(i)}=\frac{1}{r}\frac{\partial u_i}{\partial\theta}+\frac{\partial v_i}{\partial r}-\frac{v_i}{r},$$

$$\epsilon_{zz}^{(i)}=\frac{\partial w_i}{\partial z}=0; \qquad \gamma_{\theta z}^{(i)}=\frac{\partial v_i}{\partial z}+\frac{1}{r}\frac{\partial w_i}{\partial\theta}=0;$$

$$\gamma_{rz}^{(i)}=\frac{\partial u_i}{\partial z}+\frac{\partial w_i}{\partial r}=0,$$

and rotation vs displacement relations

$$2\omega_z^{(i)}=\frac{\partial v_i}{\partial r}+\frac{v_i}{r}-\frac{1}{r}\frac{\partial u_i}{\partial\theta}; \qquad 2\omega_\theta^{(i)}=\frac{\partial u_i}{\partial z}-\frac{\partial w_i}{\partial r}=0;$$

$$2\omega_r^{(i)}=\frac{1}{r}\frac{\partial w_i}{\partial\theta}-\frac{\partial v_i}{\partial z}=0,$$

and then using the stress–strain relations in terms of the stiffness constants, c_{ij}^i

$$\begin{bmatrix}\sigma_{rr}^{(i)}\\ \sigma_{\theta\theta}^{(i)}\\ \sigma_{zz}^{(i)}\\ \tau_{\theta z}^{(i)}\\ \tau_{rz}^{(i)}\\ \tau_{r\theta}^{(i)}\end{bmatrix}=\begin{bmatrix}c_{11}^i & c_{12}^i & c_{13}^i & 0 & 0 & 0\\ c_{12}^i & c_{22}^i & c_{23}^i & 0 & 0 & 0\\ c_{13}^i & c_{23}^i & c_{33}^i & 0 & 0 & 0\\ 0 & 0 & 0 & c_{44}^i & 0 & 0\\ 0 & 0 & 0 & 0 & c_{55}^i & 0\\ 0 & 0 & 0 & 0 & 0 & c_{66}^i\end{bmatrix}\begin{bmatrix}\epsilon_{rr}^{(i)}\\ \epsilon_{\theta\theta}^{(i)}\\ \epsilon_{zz}^{(i)}\\ \gamma_{\theta z}^{(i)}\\ \gamma_{rz}^{(i)}\\ \gamma_{r\theta}^{(i)}\end{bmatrix}, \quad i=f_1,c,f_2, \quad (8)$$

the buckling equations from Ref. [3] result in the following two linear homogeneous ordinary differential equations of the second-order for $U_i(r)$, $V_i(r)$, where $i=f_1$ for $R_1\le r\le R_1+f_1$; $i=c$ for $R_1+f_1\le r\le R_2-f_2$ and $i=f_2$ for $R_2-f_2\le r\le R_2$.

$$c_{11}^{(i)}U_i''+\frac{c_{11}^{(i)}}{r}U_i'-\left[\left(c_{66}^{(i)}+\frac{\sigma_{\theta\theta}^{0(i)}}{2}\right)n^2+c_{22}^{(i)}\right]\frac{U_i}{r^2} +\left(c_{12}^{(i)}+c_{66}^{(i)}-\frac{\sigma_{\theta\theta}^{0(i)}}{2}\right)\frac{nV_i'}{r}-\left(c_{22}^{(i)}+c_{66}^{(i)}+\frac{\sigma_{\theta\theta}^{0(i)}}{2}\right)\frac{nV_i}{r^2}=0, \quad (9a)$$

and

$$\left(c_{66}^{(i)}+\frac{\sigma_{rr}^{0(i)}}{2}\right)V_i''+\left(c_{66}^{(i)}+\sigma_{rr}^{0(i)}-\frac{\sigma_{\theta\theta}^{0(i)}}{2}+\frac{r\sigma_{rr}^{0(i)\prime}}{2}\right)\frac{V_i'}{r} +\left[-\left(c_{66}^{(i)}+c_{22}^{(i)}n^2+\frac{\sigma_{\theta\theta}^{0(i)}}{2}\right)+\frac{r\sigma_{rr}^{0(i)\prime}}{2}\right]\frac{V_i}{r^2} -\left(c_{12}^{(i)}+c_{66}^{(i)}-\frac{\sigma_{rr}^{0(i)}}{2}\right)\frac{nU_i'}{r} +\left[-\left(c_{66}^{(i)}+c_{22}^{(i)}+\frac{\sigma_{\theta\theta}^{0(i)}}{2}\right)+\frac{r\sigma_{rr}^{0(i)\prime}}{2}\right]\frac{nU_i}{r^2}=0. \quad (9b)$$

The associated boundary conditions are as follows.

(a) At the inner and outer bounding surfaces, we have the following two traction conditions at each of the surfaces [3]

$$\sigma_{rr}^{(j)}=0; \qquad \tau_{r\theta}^{(j)}+\sigma_{rr}^{0(j)}\omega_z^{(j)}=-p_j\omega_z^{(j)},$$

where $j=f_1$ and $p_j=0$ at $r=R_1$ (inner bounding surface) and $j=f_2$ and $p_j=p$ at $r=R_2$ (outer bounding surface),

which result in

$$c_{11}^{(j)}U_j' + \frac{c_{12}^{(j)}}{r}(U_j + nV_j) = 0, \tag{10a}$$

and

$$\left(c_{66}^{(j)} + \frac{\sigma_{rr}^{0(j)} + p_j}{2}\right)V_j' - \left(c_{66}^{(j)} - \frac{\sigma_{rr}^{0(j)} + p_j}{2}\right)\frac{V_j + nU_j}{r} = 0. \tag{10b}$$

(b) At the face-sheet/core interfaces, we have the following four conditions at each of the interfaces.

Traction continuity:

$$c_{11}^{(j)}U_j' + \frac{c_{12}^{(j)}}{r}(U_j + nV_j) = c_{11}^{(c)}U_c' + \frac{c_{12}^{(c)}}{r}(U_c + nV_c), \tag{11a}$$

and

$$\left(c_{66}^{(j)} + \frac{\sigma_{rr}^{0(j)}}{2}\right)V_j' - \left(c_{66}^{(j)} - \frac{\sigma_{rr}^{0(j)}}{2}\right)\frac{V_j + nU_j}{r} = \left(c_{66}^{(c)} + \frac{\sigma_{rr}^{0(c)}}{2}\right)V_c' - \left(c_{66}^{(c)} - \frac{\sigma_{rr}^{0(c)}}{2}\right)\frac{V_c + nU_c}{r}. \tag{11b}$$

Displacement continuity:

$$U_j = U_c; \qquad V_j = V_c, \tag{11c}$$

where $j = f_1$ at $r = R_1 + f_1$ (inner face-sheet/core interface) and $j = f_2$ at $r = R_2 - f_2$ (outer face-sheet/core interface).

2.3. Solution of the eigen-boundary-value problem for differential equations

Eqs. (9)–(11) constitute an eigenvalue problem for differential equations, with p the parameter (two point boundary value problem). An important point is that $\sigma_{rr}^{0(i)}(r)$, $\sigma_{\theta\theta}^{0(i)}(r)$ and $\sigma_{rr}^{0(i)\prime}(r)$ depend *linearly* on the external pressure, p (the parameter) through expressions in the form of Eq. (6) and this makes possible the direct application of standard solution techniques.

With respect to the method used there is a difference between the present problem and the one for the homogeneous orthotropic body solved in Ref. [3]. The complication in the present problem is due to the fact that the displacement field is continuous but has a slope discontinuity at the face-sheet/core interfaces. This is the reason that the displacement field was not defined as one function but as three distinct functions for $i = f_1, c$ and f_2, i.e. the two face-sheets and the core. Our formulation of the problem employs, hence, 'internal' boundary conditions at the face-sheet/core interfaces, as outlined above. Due to this complication, the shooting method [10] was deemed to be the best way to solve this eigen-boundary-value problem for differential equations. A special version of the shooting method was formulated and programmed for this problem. In fact, for each of the three constituent phases of the sandwich structure, we have five variables: $y_1 = U_i$, $y_2 = U_i'$, $y_3 = V_i$, $y_4 = V_i'$, and $y_5 = p$. The five differential equations are: $y_1' = y_2$, the first equilibrium equation (9a), $y_3' = y_4$, the second equilibrium equation (9b) and $y_5' = 0$.

The method starts from the inner boundary $r = R_1$ and integrates the five first-order differential equations from R_1 to the inner face-sheet/core interface $R_1 + f_1$ (i.e. through the inner face-sheet). At the inner bounding surface, R_1, we have three conditions, the two traction boundary conditions, Eq. (10), and a third condition of (arbitrarily) setting $U_{f_1} = 1.0$, therefore we have two freely specifiable variables. The freely specifiable starting values at R_1 are taken as the y_5 (pressure), and the $y_3(V_{f_1})$ and these are taken as the values from the shell theory (described later). Then, the three boundary conditions at r_1 allow finding the starting values for y_1, y_2 and y_4. Once we reach the inner face-sheet/core interface, $R_1 + f_1$, the tractions from the inner face-sheet side are calculated; these should equal the tractions from the core side, according to the boundary conditions on the face-sheet/core interface, Eqs. (11a) and (11b). This allows finding the slopes of the displacements, $y_2 = U_c'$ and $y_4 = V_c'$ for starting the shooting into the core (note that the other three functions, $y_1 = U_c$, $y_3 = V_c$ and $y_5 = p$, are continuous according to Eq. (11c), and their values at $R_1 + f_1$ have already been found at the end of the integration step through the inner face-sheet). The next step is integrating the five differential equations from $R_1 + f_1$ to $R_2 - f_2$, i.e. through the core. In a similar manner, once we reach the outer face-sheet/core interface, $R_2 - f_2$, the tractions from the core side are calculated; these should equal the tractions from the outer face-sheet side, per Eqs. (11a) and 11(b), and this allows finding the slopes of the displacements, $y_2 = U_{f_2}'$ and $y_4 = V_{f_2}'$ for starting the shooting into the outer-face-sheet (again, the other three functions are continuous and their values at $R_2 - f_2$ have already been found at the end of the integration step through the core). The third step is the integration through the outer-face-sheet. Once the outer bounding surface, R_2, is reached, the traction boundary conditions, Eq. (10), which ought to be zero, are calculated. Multi-dimensional Newton–Raphson is then used to develop a linear matrix equation for the two increments to the adjustable parameters, y_5 and y_3 at R_1. These increments are solved for and added and the shooting repeats until convergence. For the integration phase, we used a Runge–Kutta driver with adaptive stepsize control. The method produced results very fast and without any numerical complication.

3. Results

As an illustrative example, consider a sandwich ring with the following geometry: core, $c = 25.4$ mm (1 in.), face-sheets $f_1 = f_2 = f = 2.54$ mm (0.1 in.)

Sand width $B = 76.2$ mm (3 in.). This value for B was chosen in order to assume that buckling is in the plane of the ring and not out of the plane. Note that the sandwich is symmetric about its mid-surface. The total thickness of the ring is, thus, $h = 2f + c = 30.48$ mm (1.2 in.), and is kept constant. The mean radius, R_0, is chosen in such a manner that the ratio R_0/h ranges from 15 to 120.

Material properties for the face-sheets and the core are given in Table 1. The core is isotropic alloy-foam and the face-sheets are boron/epoxy or graphite/epoxy or kevlar/epoxy unidirectional with zero deg. orientation with respect to the hoop direction. Note again that 1 is the radial (r), 2 is the circumferential (θ), and 3 the axial (z) direction.

Note also that by referring to Eq. (1), the compliance constants for each orthotropic phase are:

$$a_{11} = \frac{1}{E_1}; \qquad a_{22} = \frac{1}{E_2}; \qquad a_{33} = \frac{1}{E_3};$$

$$a_{44} = \frac{1}{G_{23}}; \qquad a_{55} = \frac{1}{G_{31}}; \qquad a_{66} = \frac{1}{G_{12}},$$

$$a_{12} = -\frac{\nu_{21}}{E_2}; \qquad a_{13} = -\frac{\nu_{31}}{E_3}; \qquad a_{23} = -\frac{\nu_{32}}{E_3}.$$

3.1. Shell theory modeling

Since the shell is considered to be very long, the buckling analysis reduces to that for a ring [8]. If the transverse shear effect is neglected, the expression for the pressure becomes (classical)

$$p_{\mathrm{cl}} = 3\frac{(\mathrm{EI})_{\mathrm{eq}}}{BR_0^3}, \tag{12a}$$

where $(\mathrm{EI})_{\mathrm{eq}}$ is the equivalent bending rigidity, given in terms of the extensional moduli of the face-sheets E_{f} and the core E_{c} by:

$$(\mathrm{EI})_{\mathrm{eq}} = w\left[E_{\mathrm{f}}\frac{f^3}{6} + 2E_{\mathrm{f}}f\left(\frac{f}{2} + \frac{c}{2}\right)^2 + E_{\mathrm{c}}\frac{c^3}{12}\right]. \tag{12b}$$

If the transverse shear effect is accounted for, then

$$p_{\mathrm{w/shear}} = 3\frac{(\mathrm{EI})_{\mathrm{eq}}}{BR^3(1 + 4k_s)}; \qquad k_{\mathrm{s}} = \frac{(\mathrm{EI})_{\mathrm{eq}}}{CR_0^2}, \tag{13a}$$

where

$$C = \int_A KG\,\mathrm{d}A, \tag{13b}$$

K being a shear correction factor taken as equal to one and G is the transverse shear stiffness of the sandwich cross-section.

Two different expressions for C are employed herein. In the first case, it is assumed that only the core contributes, in which case, $C = BcG_{12}^{\mathrm{c}}$ and

$$k_{\mathrm{s1}} = \frac{(\mathrm{EI})_{\mathrm{eq}}}{BcG_{12}^{\mathrm{c}}R_0^2}, \tag{14a}$$

where G^{c} is the shear modulus of the core.

In the second case, an effective shear modulus for the sandwich section, $\bar{G}$, which includes the contribution of the facings, is derived based on the compliances of the constituent phases [11]. The expression for $\bar{G}$ is given by

$$\frac{2f + c}{\bar{G}} = \frac{2f}{G_{12}^{\mathrm{f}}} + \frac{c}{G_{12}^{\mathrm{c}}}, \tag{14b}$$

where G_{12}^{f} is the shear modulus of the facings. Therefore, in this case

$$k_{\mathrm{s2}} = \frac{(\mathrm{EI})_{\mathrm{eq}}}{B(2f + c)\bar{G}R_0^2}. \tag{14c}$$

Table 2 gives the critical pressure from the elasticity formulation for a range of mean radius over total thickness ratios, in comparison with the classical shell and the two shear deformable shell formulas. In all cases, $n = 2$ was used in the buckling modes, Eq. (9) (as is the case with external pressure). It is seen that the classical (no shear) formula can yield results highly non-conservative, even approaching 10 times the elasticity value for the lower ratio of R_0/h_{tot} and boron/epoxy case. Both shear correction formulas yield reasonable results with the shear correction formula based on the core only being in general conservative as opposed to the shear correction formula based on an 'effective shear modulus', $\bar{G}$, which is non-conservative.

In the results presented in Table 2, the face-sheets were quite thin and the shear correction formula based on the core

Table 1
Material properties

Material	E_2 (GPa)	$E_1 = E_3$ (GPa)	G_{31} (GPa)	$G_{12} = G_{23}$ (GPa)	ν_{31}	$\nu_{21} = \nu_{23}$
Face-sheets						
Boron/epoxy	221.0	20.7	3.29	5.79	0.45	0.23
Graphite/epoxy	181.0	10.3	5.96	7.17	0.49	0.28
Kevlar/epoxy	75.9	5.52	1.89	2.28	0.47	0.34
Core						
Alloy-foam (isotropic)	0.0459	0.0459	0.0173	0.0173	0.33	0.33

$1 \equiv r$, $2 \equiv \theta$, $3 \equiv z$.

Table 2
Critical pressure in N/m^2

R/h	Elasticity	Classical shell[a] no shear (% vs elast)	Shell w/shear[b] based on core only (% vs elast)	Shell w/shear[c] based on $\bar{G}$ (% vs elast)
Boron/epoxy faces w/alloy-foam core				
15	741,773	6,898,740 (+930.0%)	651,125 (−12.2%)	899,768 (+21.3%)
30	277,305	862,343 (+310.9%)	253,721 (−8.5%)	323,361 (+16.6%)
60	70,416	107,793 (+53.0%)	67,383 (−4.3%)	76,087 (+8.0%)
120	11,817	13,474 (+14.0%)	11,717 (−0.85%)	12,203 (+3.3%)
Graphite/epoxy faces w/alloy-foam core				
15	720,842	5,650,460 (+783.9%)	637,826 (−11.5%)	874,654 (+21.3%)
30	258,549	706,307 (+273.2%)	238,236 (−7.9%)	298,643 (+15.5%)
60	61,528	88,288 (+43.5%)	59,207 (−3.8%)	65,825 (+7.0%)
120	9918	11,036 (+11.3%)	9829 (−0.9%)	10,168 (+2.5%)
Kevlar/epoxy faces w/alloy-foam core				
15	605,472	2,370,590 (+391.5%)	551,668 (−8.9%)	719,856 (+18.9%)
30	171,351	296,324 (+72.9%)	162,433 (−5.2%)	188,347 (+9.9%)
60	31,418	37,040 (+17.9%)	30,712 (−2.2%)	32,397 (+3.1%)
120	4476	4630 (+3.4%)	4403 (−1.6%)	4470 (−0.13%)

Geometry: $f = 0.1$ in., $c = 1.0$ in. and $B = 3$ in.
[a] Eq. (12).
[b] Eq. (14a).
[c] Eqs. (14b) and (14c).

only, Eq. (14a), seemed to be more accurate. In order to further examine this premise, the critical load was calculated for a construction in which the total thickness remains the same but the face-sheet thickness is increased at the expense of the core. The results, listed in Table 3, show that the shear correction formula based on an effective modulus (which includes the core), Eqs. (14b) and (14c), is now more accurate.

3.2. Finite element modeling

The ABAQUS [12] finite element code was used for this part of the research. Two types of elements were used: (i) shear deformable shell elements and (ii) solid 3D (brick) elements.

Regarding (i), the 'thick shell' element S8R was used. This is an eight-node element with reduced integration and it allows large rotations (and small strains). Due to the symmetry at $\theta = 0°$ and the anti-symmetry at $\theta = 45°$, only one-eighth of the ring need be modeled (a 45° sector). This part was meshed with 32 elements. A convergence study showed that no more elements are needed.

Regarding (ii), the 3D 'brick' element C3D20R was used. This is a 20-node reduced integration element. A 90° sector was meshed with 48 by 2 elements. At $\theta = 0°$ and at $\theta = 90°$ there are symmetry boundary conditions. Again, a convergence study showed that no more elements are needed.

The results are shown in Table 4. The results from both the shell and the solid 'brick' elements follow the same trends. Shell elements give results which are close to the shear deformable shell theory formula, and the solid brick elements give results which are closer to the elasticity solution presented herein. Even in the most demanding case of $R/h = 15$, the finite element results with solid elements are about 6% higher than the benchmark elasticity solution. But with shear deformable shell elements, the results are about 10% above the elasticity value. On the contrary, the shell theory formula is about 20% above the elasticity value. These differences get smaller as the ratio R/h is increased, i.e. for thinner shells.

Table 3
Critical pressure in N/m^2

R/h	Elasticity	Classical shell no shear (% vs elast)	Shell w/shear based on core only (% vs elast)	Shell w/shear based on $\bar{G}$ (% vs elast)
Graphite/epoxy faces w/alloy-foam core				
15	1,244,010	11,731,900 (+943.1%)	416,091 (−66.6%)	1,501,160 (+20.7%)
30	393,573	1,466,490 (+372.6%)	188,038 (−52.2%)	542,378 (+37.8%)
60	105,699	183,311 (+73.4%)	67,900 (−35.8%)	128,553 (+21.6%)
120	19,297	22,914 (+18.7%)	16,081 (−16.7%)	20,709 (+7.3%)

Effect of increased face thickness: $f = 0.3$ in., $c = 0.6$ in. and $B = 3$ in.

Table 4
Critical pressure in N/m^2: comparison with finite element results

R/h	Elasticity	Shell w/shear based on $\bar{G}$ (% vs elast)	S8R FE (% vs elast)	C3D20 FE (% vs elast)
Boron/epoxy faces w/alloy-foam core				
15	741,773	899,768 (+21.3%)	809,208 (+9.1%)	783,556 (+5.6%)
30	277,305	323,361 (+16.6%)	298,839 (+7.8%)	287,722 (+3.7%)
60	70,416	76,087 (+8.0%)	73,863 (+4.8%)	72,373 (+2.7%)
120	11,817	12,203 (+3.3%)	12,189 (+2.9%)	12,106 (+2.2%)
Graphite/epoxy faces w/alloy-foam core				
15	720,842	874,654 (+21.3%)	790,739 (+9.7%)	762,926 (+5.8%)
30	258,549	298,643 (+15.5%)	278,606 (+7.8%)	268,754 (+3.9%)
60	61,528	65,825 (+7.0%)	64,381 (+4.6%)	63,244 (+2.8%)
120	9918	10,168 (+2.5%)	10,184 (+2.6%)	10,126 (+2.0%)
Kevlar/epoxy faces w/alloy-foam core				
15	605,472	719,856 (+18.9%)	673,845 (+11.3%)	647,488 (+7.0%)
30	171,351	188,347 (+9.9%)	184,090 (+7.5%)	179,624 (+4.8%)
60	31,418	32,397 (+3.1%)	32,633 (+4.0%)	32,341 (+3.1%)
120	4476	4470 (−0.13%)	4533 (+2.3%)	4522 (+2.0%)

4. Conclusions

An elasticity solution to the problem of buckling of sandwich long cylindrical shells subjected to external pressure is presented. The results from this solution are compared with (i) shell theory results with and without accounting for the transverse shear effect and (ii) finite element results by use of the ABAQUS finite element code and using two types of elements: a shear deformable shell element and a solid 3D (brick) element. In this study all constituent phases of the sandwich structure, i.e. the facings and the core, are assumed to be orthotropic and the loading is a uniform hydrostatic pressure, which means that the loading remains normal to the deflected surface during the buckling process. Results are produced for laminated facings, namely, boron/epoxy, graphite/epoxy and kevlar/epoxy laminates with zero deg. orientation with respect to the hoop direction, and for alloy-foam core. The results show that the shell theory predictions without transverse shear can produce highly non-conservative results on the critical pressure. The elasticity solution presented herein provides a means of accurately assessing the limitations of shell theories in predicting stability loss in sandwich shells.

Acknowledgements

The financial support of the ONR's Research Program on 'Composites for Marine Structures', Grants N00014-90-J-1995 and N00014-0010323, and the interest and encouragement of the Program Manager, Dr Yapa D.S. Rajapakse, are both gratefully acknowledged.

References

[1] Librescu L. Elastostatics and kinetics of anisotropic and heterogeneous shell-type structures. Leyden: Nordhoff International; 1975.
[2] Reddy JN, Liu CF. A higher-order shear deformation theory of laminated elastic shells. Int J Engng Sci 1985;23(3):319–30.
[3] Kardomateas GA. Buckling of thick orthotropic cylindrical shells under external pressure. J Appl Mech (ASME) 1993;60:195–202.
[4] Kardomateas GA, Chung CB. Buckling of thick orthotropic cylindrical shells under external pressure based on non-planar equilibrium modes. Int J Solids Struct 1994;31(16):2195–210.
[5] Kardomateas GA. Benchmark three-dimensional elasticity solutions for the buckling of thick orthotropic cylindrical shells. Composites Part B 1996;27B:569–80 [Special issue on 'Thick Composites'].
[6] Lekhnitskii SG. Theory of elasticity of an anisotropic elastic body. San Francisco/Moscow: Holden Day/Mir Publishers; 1981.
[7] Kardomateas GA. Elasticity solutions for a sandwich orthotropic cylindrical shell under external pressure, internal pressure and axial force. AIAA J 2001;39(4):713–9.
[8] Smith Jr CV, Simitses GJ. Effect of shear and load behavior on ring stability. ASCE J EM Div 1969;95(EM3):559–69.
[9] Simitses GJ, Aswani M. Buckling of thin cylinders under uniform lateral loading. J Appl Mech (ASME) 1974;41(3):827–9.
[10] Press WH, Flannery BP, Teukolsky SA, Vetterling WT. Numerical recipes. Cambridge: Cambridge University Press; 1989.
[11] Huang H, Kardomateas GA. Buckling and initial postbuckling behavior of sandwich beams including transverse shear. AIAA J 2002;40(11):2331–5.
[12] ABAQUS. Providence, RI: Hibbit, Karlsson and Sorensen Inc.; 1971.